Proceedings of ASME Turbo Expo 2012
GT2012
June 11-15, 2012, Copenhagen, Denmark

GT2012-70056

INFLUENCE OF WETNESS ON EFFICIENCY OF THE FULL SCALE SIZE LOW PRESSURE TURBINES

Tomohiko Tsukuda, Hiroyuki Kawagishi, Naoki Shibukawa, Tadayuki Hashidate, Koichi Goto
Power and Industrial Systems Research and Development Center
Toshiba Corporation
Yokohama 230-0045, Japan
Email: tomohiko.tsukuda@toshiba.co.jp

Tsuguhisa Tashima
Keihin Product Operations, Toshiba Corporation
Yokohama 230-0045, Japan

ABSTRACT

Efficiencies of 60Hz full size test turbines were measured in various wet steam conditions to reveal the wetness impact on the performance. We changed the wetness and stage load conditions independently under the condition of constant steam mass flow rate in the low pressure turbine. The test results told that the stage efficiency decreases with the increasing of wetness as many studies showed, furthermore, the stage efficiency decreases more in smaller load conditions than in the design point. In addition, blade length effects were examined by comparing two types of LP turbine to be found that the longer case got more deficits at the same wetness. Some theoretical evaluations were tried and a combination of some simple loss models explained the tendencies above, qualitatively. The evaluation showed that absolute value of mechanical wet loss such as braking loss remained unchanged regardless of load conditions, so in low load condition, ratio of mechanical loss to stage load increased, resulting decrease of stage efficiency. It also showed that increasing wet loss at the longer blade was mainly because higher circumferential velocity caused larger mechanical wet loss such as braking loss.

INTRODUCTION

The steam in low pressure steam turbines operating in thermal power plants is generally expanded to a vacuum, and the turbine exit operates in wet-steam conditions. In geothermal and nuclear power plants, almost all the turbine stages operate in wet steam because the inlet steam temperature is lower than that of thermal power plants. The wet steam includes various sizes of fog droplets, which will influence the performance and the reliability of the steam turbine [1]. The wet steam also influences the flow discharge coefficient, which is affected by super saturation phenomena and the wetness fraction [2].

Moisture loss in steam turbines has been examined by many authors. Early work by Baumann suggested that 1% wetness present in a stage was likely to cause 1% decrease in stage efficiency [3]. Miller et al. studied the relationship between turbine efficiency and average wetness fractions using a full size test turbine [4]. Gyarmathy proposed some simplified expressions for the different losses caused by fog droplets and the water film [5]. Young reported many studies on the characteristics of wet steam flow [6]-[9]. More recently, by means of enhanced wet analysis CFD codes, a lot of simulation researches with a large size and complex analysis model have been performed. Yamamoto et al. investigated unsteady 3-D flows through two-stage stator-rotor cascade in a low-pressure steam turbine model numerically and experimentally assuming dry and wet-steam conditions [10]. Starzmann et al. compared the calculated flow pattern both by homogeneous and heterogeneous condensation with the results of the test turbine and concluded the former was likely to give better simulation [11].

The principle of similarity is sometimes not applicable as for the moisture loss. For example, moisture droplet size in steam is thought to be independent of the turbine scale. It means the moisture loss measured by scale model turbine tests cannot be directly applied to the design of actual machines because the relative impact of the droplet to the flow and blade rows is different. Therefore, experiments of the actual size

turbine are strongly desired. Recently, Shibukawa et al. implemented a series of full size turbine test [12]. In this paper, Influence of wetness on efficiency of the full scale size low pressure turbines is investigated as a part of the tests above. Wetness and stage load condition are varied independently under the condition of constant steam mass flow late. By comparing two types of LP turbine efficiency, blade length effects on moisture loss are also evaluated. Further, with the use of some physics-based moisture loss model, we try to explain the difference of deficit between two types of LP turbines.

NOMENCLATURE

D	droplet diameter (m)
G	steam flow rate (kg/s)
G_w	flow rate of droplets (kg/s)
h	enthalpy (J)
L_a	acceleration loss (W)
L_b	braking loss (W)
L_{bear}	bearing loss (W)
L_m	moisture loss (W)
L_p	pumping loss (W)
p	pressure (Pa)
P_{gen}	generator power output (W)
S	entropy (J/K)
t	temperature (K)
U	blade velocity (m/s)
U_o	outer blade velocity (m/s)
U_d	blade velocity where droplets deposited (m/s)
V	droplet velocity at leading edge of blade (m/s)
W	relative velocity (m/s)
W_{imp}	droplet impact relative velocity (m/s)
We	Weber number
Y	L0 nozzle exit wetness

Greek symbols

α_{ana}	analytical moisture loss coefficient
α_{exp}	experimental moisture loss coefficient
α_{eff}	negative gradient of overall efficiency along with L0 nozzle exit wetness
η	efficiency
ρ	density (kg/m^3)
σ	droplet surface tension (N/m)

Subscript

L-0,1,2,3,4,5	last stage, 1,2,3,4,5 stage upstream
in	inlet
out	outlet
is	isentropic
i	droplet number

EXPERIMENTAL METHOD

Experimental Facility

The measurements were performed in the full scale LP turbines at the actual size steam turbine development facility "Mikawa Power Station Unit-2". Figure 1 describes the configuration of the facility. The facility was built adjacent to a conventional coal fired power plant, which shares utilities like a boiler, piping, heat exchanger, etc. The turbine arrangement is cross compound in which HP and LP turbines have separate generators on their axles, which enable accurate performance measurement and precise evaluation. The mechanical layout of this facility is based on the concept that HP and LP turbines can be replaced independently. A more detailed description of the test facility is available in Shibukawa et al [12].

Two types of LP turbines were installed in the No.2 turbine unit and investigated. One is named 35" LP turbine and the other is named 48" LP turbine in this paper. Both turbines were representative of a typical low pressure section of steam turbine for power generation plant. Figure 2 shows the overview of assembled 48" LP turbine. The specifications of the both turbines are shown in Table 1. Basic configuration of each turbine such as number of stages and LP section power output are same. The primary differences between two turbines are blade length of the last stage as shown in table1. Blades length of L-1 and L-2 of 48" LP turbine are also longer than those of 35" LP turbine as shown in Table 2.

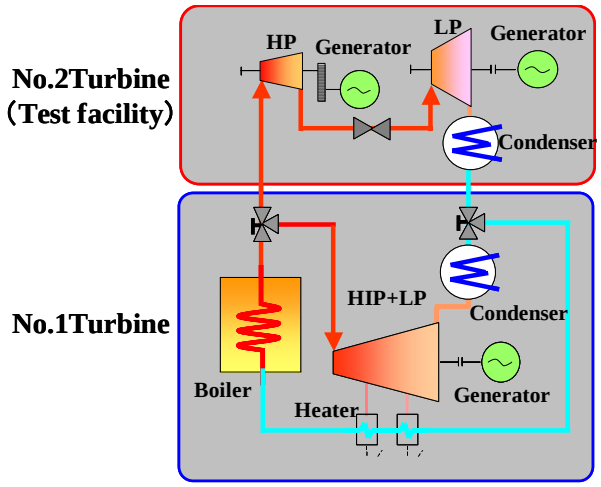

HP:High Pressure Turbine
LP:Low Pressure Turbine
HIP:High Pressure/Intermediate Pressure Turbine

Figure 1 Configuration of the test facility

Table 1 Model turbines features

	35" LP turbine	48" LP turbine
Rotor speed [RPM]	3600	3600
Number of stages	6	6
L-0 Blade length [mm]	889	1219.2

Table 2 Blade height ratio of 48" LP turbine to 35" LP turbine

	L-2	L-1	L-0
Blade length ratio	1.15	1.13	1.37

Figure 2 Overview of assembled 48” LP turbine

Test Conditions

Table 3 shows main parameters of the current study. The LP inlet temperature is set at 200 to 350 ^{o}C for both 35” LP turbine and 48” LP turbine, providing wide range of wetness conditions. The back pressure of LP turbine is set at 4.4-7.4 kpa for 35” LP turbine and 4.4-7.9 kpa for 48” LP turbine respectively to set wide range of exhaust axial velocity. Figure 3 shows a schematic expansion lines to explain maximum and minimum wetness conditions. There are two ways to control the LP inlet temperature in the facility. One is to control the boiler outlet temperature. The other is to control the HP turbine outlet pressure by controlling the valve located in the downstream of HP turbine exhaust. By the ways above, natural steam condition that is generated by steam expansion can be supplied to the LP turbine with no desuperheater. The LP exhaust pressure is precisely controlled by the operation of cooling tower and the air flow rate into the condenser to cover the wide exhaust velocity range. Boiler load was kept constant through the all test case. Steam mass flow rate of LP turbine slightly increases in the amount of boiler superheater splay which controls the boiler outlet temperature. Steam mass flow rate is with a range of 7% through the all test condition.

Table 3 Main parameters of the current study

	35" LP turbine	48" LP turbine
Turbine inlet temperture [℃]	200-350	200-350
Back pressure [kpa]	4.4-7.4	4.4-7.9

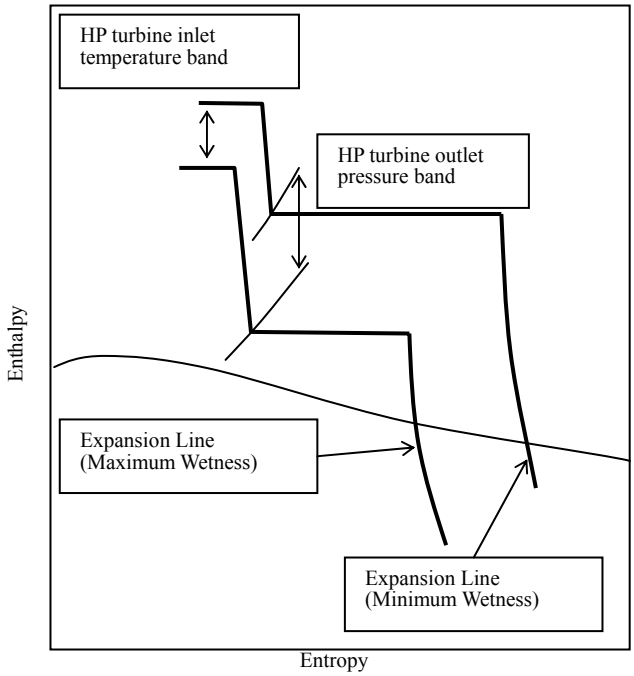

Figure 3 Conceptual h-s Chart of Mikawa Turbine Test Facility

Measurement Instruments

Figure 4 shows the traverse probe layout of the 35” LP turbine. In this study, pressure and temperature measurements in the flow path ware taken to evaluate the LP turbine overall efficiency and each stage efficiency. Rake probes are installed at LP section inlet, L2 inlet, L1 inlet, L0 inlet and L0 outlet and 4 rake-probes are arranged circumferentially at each axial position in the LP turbine. In addition, traverse measurement points are arranged between L2 inlet and L0 outlet of LP turbine where traverse actuators are mounted on LP turbine. The example of rake probe and the traverse measurement devices are shown in Figure 5. Usually 5-hole probe and thermocouple are installed in the devices for the flow pattern measurement, while the special probes such as bore scope are also applied according to the objective of the test. The pressure scanner provided for the LP turbine has a purge system because it will be operated in wet steam conditions.

To clarify the L0 exhaust enthalpy which is below saturation point, LP turbine generator output, LP turbine steam mass flow rate and mechanical loss such as bearing loss were also measured accurately. Independent LP turbine generator can help increasing the precision of measurement. The accuracy of measured data of electrical power meter is 0.2% for generator power output. The total uncertainty in the efficiency by measurement error including temperature, pressure, and condensed water flow measurement is in the order of 0.4% in this paper.

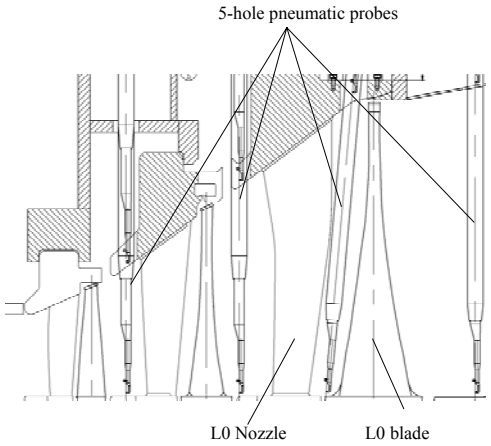

Figure 4 Traverse probe layout of the 35” LP turbine

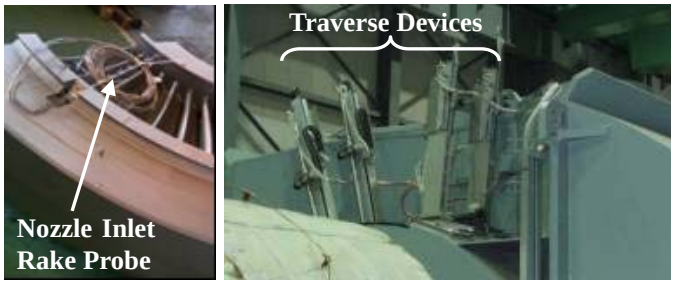

Figure 5 Measurement Instruments for LP turbine

RESULTS AND DISCUSSION

At first, we present the experimental results of 35” LP turbine and 48” LP turbine. Then, we explain some physics-based moisture loss model and discuss about comparison between the experimental results and analytical results.

Experimental Results

Figure 6 and 7 show the overall efficiency for various wetness and back pressure in 35” LP turbine and 48” LP turbine, respectively.

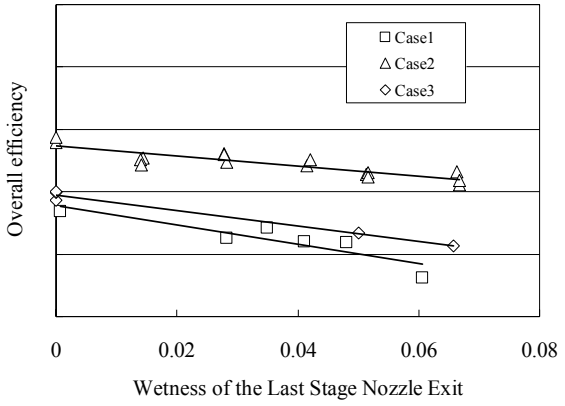

Figure 6 Overall efficiency with various wetness and back pressure in the 35” LP turbine

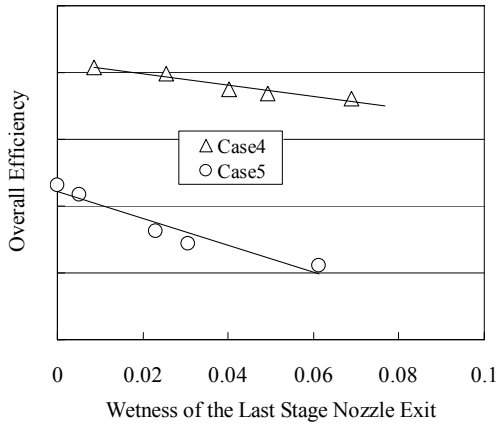

Figure 7 Overall efficiency with various wetness and back pressure in the 48” LP turbine

$$\eta_{overall} = \frac{h_{L5\ in} - h_{L0\ out}}{h_{L5\ in} - h_{L0\ out\ is}} = \frac{(P_{gen} + L_{bear})/G}{h_{L5\ in} - h_{L0\ out\ is}}$$

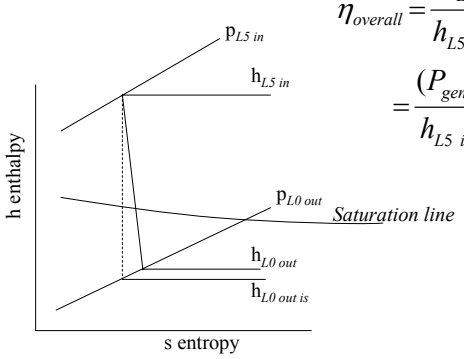

Figure 8 Overall efficiency calculation

Table 4 Back pressure condition of each case

		Back pressure (kpa)
Case1	35” LP turbine	4.4
Case2	35” LP turbine	6.2
Case3	35” LP turbine	7.4
Case4	48” LP turbine	4.4
Case5	48” LP turbine	7.9

Figure 8 shows Overall efficiency calculation. Where, $h_{L5\ in}$ is calculated from measurement values of $t_{L5\ in}$ and $p_{L5\ in}$, $h_{L5\ out\ is}$ is calculated from measurement values of $t_{L5\ in}$, $p_{L5\ in}$ and $p_{L0\ out}$, $h_{L0\ out}$ can not be calculated directly from temperature measurement because expansion line exceeds the saturation line all the test cases. Therefore, $h_{L0\ out}$ is evaluated using generator output, bearing loss and steam flow rate as shown in Figure 8. Table 4 shows the back pressure conditions of each Case. Case1, 2, 3 are for the 35” LP turbine. Case 4 and

5 are for the 48” LP turbine. For all cases LP turbine mass flow rate is almost constant and LP inlet temperature are varied from 200 to 350℃.

It can be seen that overall efficiency decreases with the increasing of the wetness of the L0 nozzle exit as many studies showed. Efficiency level also decreases with the increasing of back pressure. The increasing of back pressure of Case 2, 3 and 5 leads to lower axial exhaust velocity of L0 stage than that of design point, which deteriorate of L0 efficiency by increasing of windage loss resulting the deficit of the overall efficiency.

For figure 6 and 7, absolute values of vertical axis is our vendors confidential and can not be presented in this paper. For the perspective of wetness effect on the performance of LP turbine, however, negative gradient of overall efficiency along with the wetness is key factor and relative comparison of those parameters is discussed bellow. Figure 9 shows the normalized negative gradients of overall efficiency along with the wetness of the L-0 nozzle exit α_{eff} at each case. α_{eff} is a coefficient of linear approximate equation of efficiencies at each case and is normalized with that of Case1. α_{eff} increases with the increasing of the back pressure for both 35” LP turbine and 48” LP turbine. By comparison of 35” LP turbine and 48” LP turbine, α_{eff} of 48” LP turbine are larger than that of 35” LP turbine.

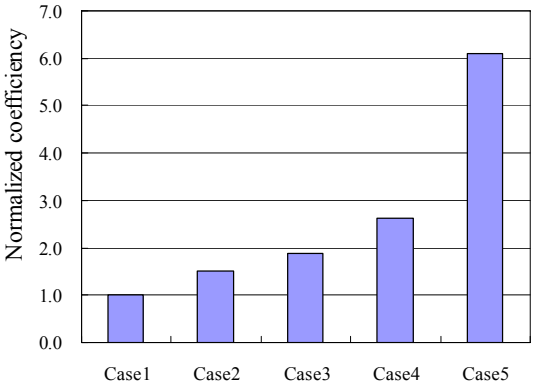

Figure 9 Normalized negative gradients of overall efficiency along with the wetness α_{eff} at each case

α_{eff} consists of not only moisture loss coefficient α_{exp} but also the variation of the each stage dry efficiency with the velocity ratio and the effect of moving expansion line which affects the LP overall efficiency. Therefore, it is important to separate the moisture loss coefficient from those factors.

Figure 10 and 11 show the normalized dry efficiency of the L5-L3 with various range of velocity ratio in 35” LP turbine and 48” LP turbine, respectively. Figure 12 shows L5-L3 efficiency calculation.

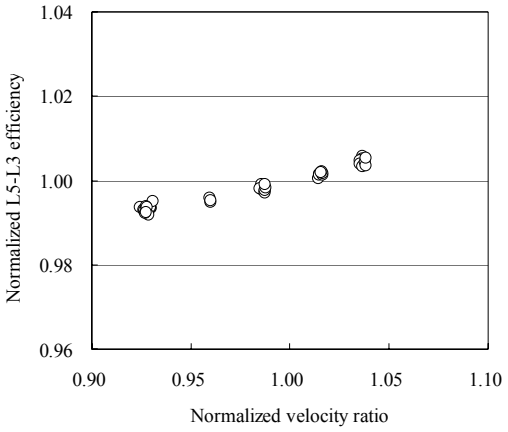

Figure 10 Non dimensional L-5-L-3 efficiency with normalized velocity ratio in 35” LP turbine

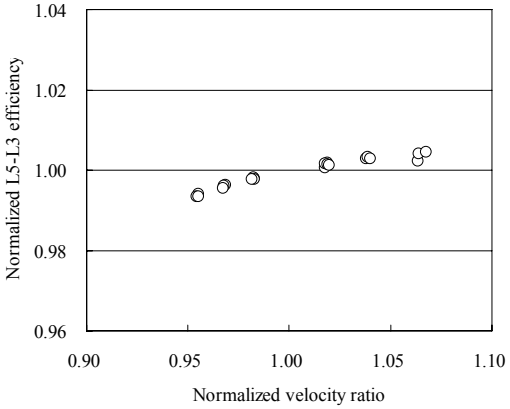

Figure 11 Non dimensional L-5-L-3 efficiency with normalized velocity ratio in 48” LP turbine

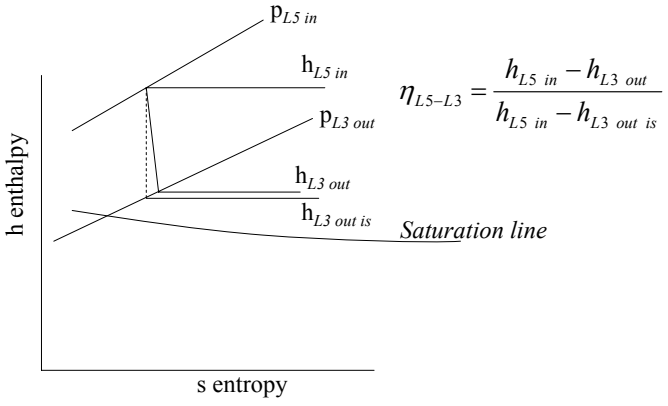

Figure 12 L5-L3 efficiency calculation

For L5-L3 efficiency, $h_{L5\ in}$, $h_{L3\ out\ is}$ and $h_{L3\ out}$ are all calculated from measurement values of temperature and pressure because expansion line does not exceed the saturation line. Velocity ratio is defined as rotational speed of blade divided by the heat drop and it is normalized by the design velocity ratio in Figure 10 and 11.

It can be found that with increase of velocity ratio the efficiency of L5-L3 increases in both 35" LP turbine and 48" LP turbine. In this test condition, the lower LP inlet temperature leads to deeper wetness condition and smaller heat drop of each stage while constant rotational speed of blades resulting higher velocity ratio. Therefore, as wetness of L0 nozzle exit increases efficiency of L5-L3 increases. The effect has positive influence on α_{eff}.

Figure 13 shows concept of moving expansion lines with LP inlet temperature in h-s chart. The length of expansion line in the maximum wetness condition is shorter than that of minimum wetness condition. Therefore, even if each stage efficiency is assumed to be same in minimum wetness condition and maximum wetness condition, the overall efficiency of the minimum wetness condition is higher than that of maximum wetness condition. The effect has negative influence on α_{eff}.

The moisture loss coefficient α_{exp} can be obtained by deducting the two effects mentioned above from α_{eff}. Figure 14 shows comparison of α_{eff}, α_{exp}, and the two effects mentioned above. In each case, Summation of 3 bars on the right side equal to α_{eff}. Magnitude relation between α_{eff} and α_{exp} among Case1 to Case5 is unchanged. Further discussion based on the physics is implemented in the next chapter with the comparison with the analytical results.

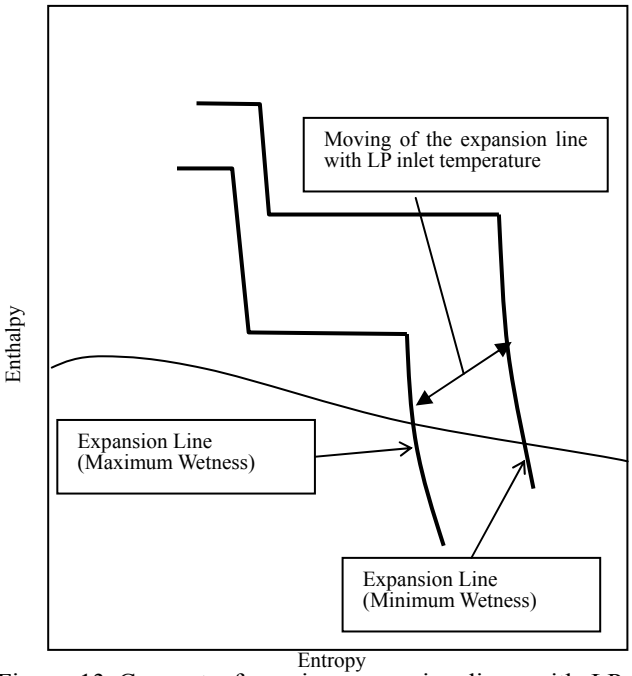

Figure 13 Concept of moving expansion lines with LP inlet temperature in h-s chart

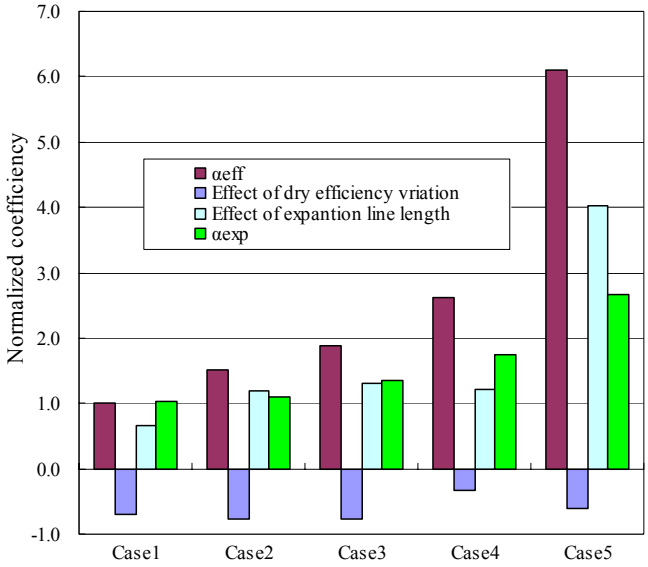

Figure 14 Comparison of α_{eff}, Effect of dry efficiency variation, Effect of expantion line length, and α_{exp}

Analytical investigation

To understand more about moisture loss, moisture loss calculations using physics-based moisture loss model are implemented in this chapter.

Generally, for the low wetness fractions the thermodynamic moisture losses such as super saturation loss are dominant factor in the moisture loss. On the other hand, for the deep wetness faction, the thermodynamic moisture loss is relatively reduced and mechanical moisture loss such as acceleration loss and braking loss becomes more dominant.

Thermodynamic moisture loss may cause sharp decrease of efficiency around the low wetness fractions. In both Figure 6 and 7, however, it can not be seen and gradient of efficiency along with the wetness is almost constant in wide range of wetness. Our recognition is that almost thermodynamic loss is probably occurred even if the driest test condition because turbine exit condition is still below saturation line. In other words, overall efficiency at all cases may already include almost thermodynamic loss. Therefore, we consider that the experimental moisture loss coefficient is mainly due to mechanical moisture loss and only mechanical moisture loss models such as braking loss are used for the analysis for simplicity.

Figure 15 shows the moisture loss calculation flow used in this paper. At first we implemented the 1-dimetional calculation to reveal each stage inlet and outlet condition. When the steam condition is below the saturation point, identification of enthalpy can not be achievable by the measured temperature and pressure. Therefore, 1-dimetional

calculation is required. 1-dimensional calculation code which was used in this study was modified to correspond to the test results. Then, we evaluate the nozzle outlet condition by using an in-house CFD code which was a blade-to-blade FVM (Finite Volume Method) code. A structured mesh with about 0.1 million points for one stage was used and the Baldwin-Lomax turbulence model is integrated into the code, which was assumed to be practical for various cases. In the present study, this code was used to examine nozzle exit radial distribution of each quantity for each stage.

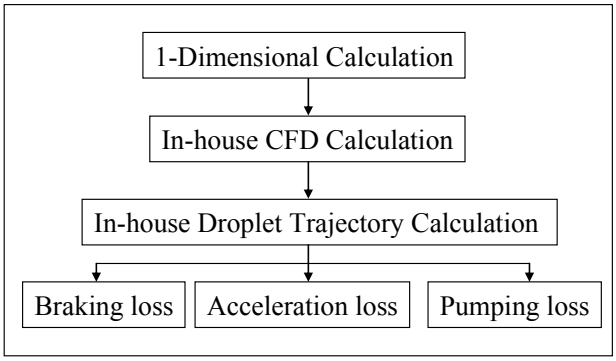

Figure 15 Moisture loss calculation flow used in the paper

Figure16 presents one of the stationary pictures cut out of the digital movie taken by the bore scope, which is focusing on the last stage nozzle surface of suction side at about 50% height. It is clearly observed that several discrete water streams come together at the trailing edge to form a water film due to water surface tension along the span-wise direction, which should atomize large size water droplets downstream.

In the droplet trajectory calculation, a domain between nozzle trailing edge and blade leading edge was divided to finite domains in the radial direction. In each divided domain, state quantities of steam phase are assumed to be constant, which is obtained from the CFD above. Figure 17 shows typical water mass fraction in the nozzle trailing edge in the radial direction which is used in this calculation. This distribution was obtained from our company's model turbine tests. The water droplets are accelerated by the gas-phase momentum and moves in the radial direction by the centrifugal force of itself. The droplet size on the nozzle trailing edge is estimated by using an equation as follows.

$$D = \frac{We\sigma}{\rho W^2} \qquad (1)$$

Where *We* is Weber number, σ is droplet surface tension, ρ is density, *W* is relative velocity. Critical Weber number of 23 is assumed to obtain maximum droplet size. Number of each size droplet is assumed to follow the normal distribution.

Figure 18 describes typical water droplet trajectories from the trailing edge of nozzle to the leading edge of bucket. Larger droplets tend to move a radial direction than smaller droplet because centrifugal force becomes more dominant for larger droplet. By this calculation, we obtained the droplet impact relative velocity and water mass fraction distribution in the radial direction on the leading edge of the moving blade locally, which enable to evaluate the mechanical loss by summate all the droplet state quantity at the leading edge of the moving blade.

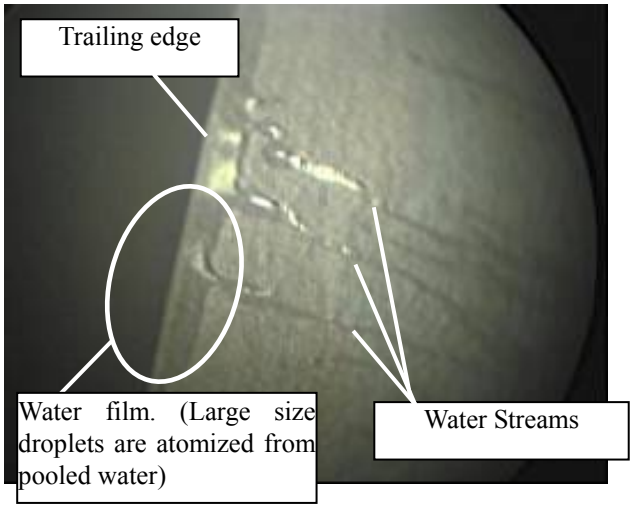

Figure 16 Water stream on the L-0 nozzle surface

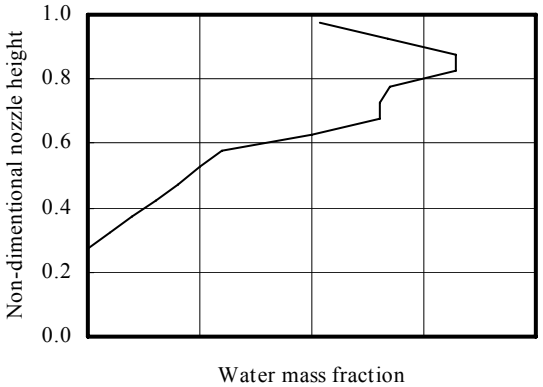

Figure 17 Distribution of water mass fraction of L0 nozzle trailing edge

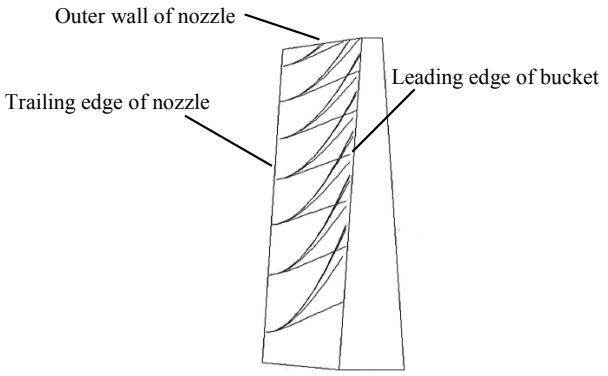

Figure 18 Typical water droplet trajectories from the trailing edge of nozzle to the leading edge of bucket

Braking loss

The large droplets from the trailing edge of the nozzle impact on the leading edge of the moving blades, which reduce the blade work due to a braking effect. The braking loss L_b is calculated as follows:

$$L_b = \sum_i G_{w\,i} U_i W_{imp\,i} \quad (2)$$

Where G_w is the flow rate of droplets, U is the blade velocity, W_{imp} is the droplet impact relative velocity, i is number of droplets.

Acceleration loss

The water deposited on the stationary blades forms liquid films which are torn off from the trailing edges and produce relatively large droplets. Since the large droplets are accelerated by the main flow, an acceleration loss is produced.

The acceleration loss L_a is calculated as follows:

$$L_a = \sum_i \frac{1}{2} G_{w\,i} V_i^{\,2} \quad (3)$$

Where G_w is the flow rate of droplet, V is droplet velocity at leading edge of moving blade, i is number of droplets.

Pumping loss

On the moving blade, the deposited water moves in the radial direction towards the blade tip by centrifugal force, which reduces the blade work due to a pumping effect.

The pumping loss L_p is calculated as follows:

$$L_p = \sum_i G_{w\,i} \left(U_o^2 - U_{d\,i}^2 \right) \quad (4)$$

Where G_w is the the flow rate of droplets deposited on the surface of the moving blade, U_O is the outer blade velocity, U_d is the blade velocity where droplets deposited, i is number of droplets.

Figure 19 shows the relative comparison of analytical moisture loss of 35" LP turbine and that of 48" LP turbine. The results are calculated for the maximum wet condition in Case 1 for 35" LP turbine and for the maximum wet condition in Case 4 for 48" LP turbine. The loss is sum of the braking loss, accelerating loss and pumping loss of L2, L1 and L0 stages. The moisture loss of 48" LP turbine are about 1.7 times larger than that of 35" LP turbine.

Figure 20 shows the comparison of experimental moisture loss coefficient and analytical moisture loss coefficient. Analytical moisture coefficient are calculated by the equation as follows

$$\alpha_{ana} = \frac{L_m}{GY(h_{L5\ in} - h_{L0\ out\ is})} \quad (5)$$

Where L_m is moisture loss, G is the steam mass flow rate, Y is L-0 nozzle exit wetness.

From Case 1 to Case 3, L_m is assumed to be constant because L0 choking is maintained and upstream of L-0 nozzle exit condition is unchanged. From Case 4 to Case 5, L_m is also assumed to be constant due to same reason. Magnification of analytical moisture loss coefficients are corrected uniformly so that analytical moisture loss coefficient corresponds to experimental moisture loss coefficient in the Case1. From Case1 to Case3, tendency of experimental moisture loss coefficients and analytical moisture loss coefficients corresponds well, which indicate that absolute value of mechanical moisture loss such as pumping loss and braking loss are constant as long as L0 nozzle exit condition is unchanged. In this circumstance, it can be said that moisture loss coefficient is almost inversely proportional to isentropic heat drop of LP turbine.

Comparison of Case1 and Case4 which are at the almost same isentropic heat drop, tendency of experimental moisture coefficient and analytical moisture loss coefficient also corresponds well. Braking loss and pumping loss increases with the increasing tip blades rotating speed of 48" LP turbine in the analytical result. It indicates that effects of the blade length on the moisture loss are explainable on the basis of mechanical moisture loss such as braking loss and pumping loss.

Comparison of Case4 and Case5 shows that there is a disagreement of tendency between experimental coefficients and analytical coefficient. Case 5 is in the very low exhaust axial velocity condition, namely off-design condition. Figure 21 shows the stream line of L-0 stage in Case 5 calculated by CFX code. It can be seen that large reverse flow region occurs in the blade region. Under the circumstances, water droplet may comes from exit of L-0 stage in the hub region, which possibly increasing the pumping loss of L-0 blade. It can make it difficult to predict moisture loss in the off-design condition.

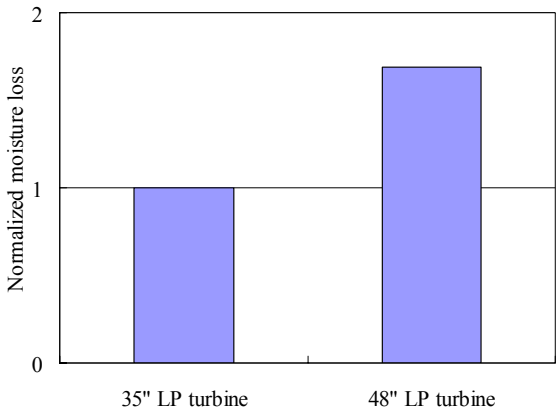

Figure 19 Comparison of analytical moisture loss of 35” LP turbine and 48” LP turbine

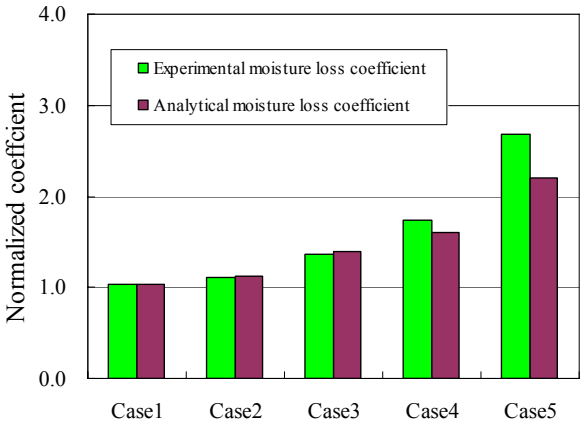

Figure 20 Comparison of experimental moisture loss coefficient and analytical moisture loss coefficient

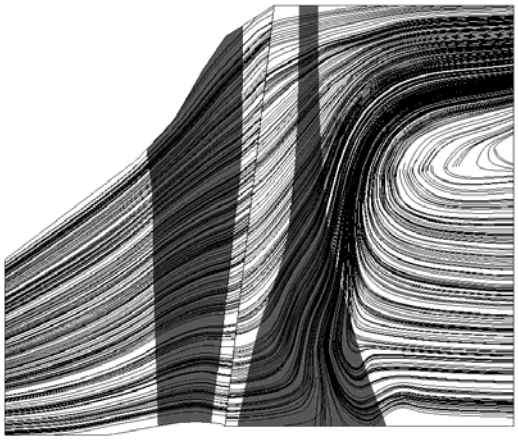

Figure 21 Stream line of L-0 stage in Case 5

CONCLUSIONS

Efficiencies of 60Hz full size test turbines were measured in various wet steam conditions to reveal the influence of wetness on efficiency of the full scale size low pressure turbines.

Influence of back pressure on moisture loss was examined. Moisture loss coefficient increases with the increasing of the back pressure for both 35” LP turbine and 48” LP turbine. Tendency of experimental moisture loss coefficients and analytical moisture loss coefficients corresponds well. It indicates that absolute value of mechanical moisture loss such as pumping loss and braking loss are constant as long as L0 choking is maintained. In this circumstance, it can be said that moisture loss coefficient is almost inversely proportional to isentropic heat drop of LP turbine.

Blade length effects on the moisture loss were examined by comparing 35” LP turbine and 48” LP turbine. Experimental moisture loss coefficient of 48” LP turbine is about 1.7 times larger than that of 35” LP turbine. Comparison of experimental results and analytical results indicates that effects of the blade length on the moisture loss are explainable on the basis of mechanical moisture loss model such as braking loss and pumping loss.

REFERENCES

[1] Nagao, S., 1986, “Behavior and influence of wet steam in a steam turbine”, Turbomachinery, Vol.14, No.6, pp.13-20.

[2] Kawagishi, H., 1994, “Some problems and countermeasures of mixed-phase flow in a steam turbine”, Turbomachinery, Vol.22, No.11, pp.53-60.

[3] Baumann, K.,1921 “Some Recent Developments in large steam turbine practice”, Journal of Institution of Electrical Engineers, Vol.59, pp.565-663.

[4] Miller E H, Schofield, P., 1972 “The performance of large steam turbine generators with water reactors”, ASME Winter Meeting.

[5] Gyarmathy, G., 1964 “Foundation of a theory of the wet-steam turbine” FTD-TT-63-785.

[6] Young, J B., 1984 “Semi-analytical techniques for investigating thermal non-equilibrium effects in wet steam turbines”, International Journal of Heat and Fluid Flow, Vol.5, No.2, pp.81-91.

[7] Young J B, Yau, K K., 1988, “The inertial deposition of fog droplets on steam turbine blades”, Journal of Turbomachinery, Vol.110, pp.155-162.

[8] Young J B, Yau K K, Walters, P T., 1988, “Fog droplet deposition and coarse water formation in low-pressure steam turbines: a combined experimental and theoretical analysis”, Journal of Turbomachinery, Vol.110, pp.163-172.

[9] Young, J B., 1995, “Wet-steam research at Cambridge 1980-1995”. EPRI Workshop on Moisture Nucleation in Steam Turbines, pp.1-15.

[10] Yamamoto, S., Sasao, Y., Kato, H., 2010, “Numerical and Experimental Investigations of Unsteady 3-D Wet-Steam Flows Through Two-Stage Stator-Rotor Cascade Channels” ASME GT2010-22796
[11] Starzmann, J., Schatz, M., Casey, M.V., Mayer, J.F., 2011, “Modeling and validation of Wet Steam Flow in a Low Pressure Steam Turbine”, ASME GT2011-45672
[12] Shibukawa, N., Kawasaki, S., Kawakami, H., Okuno, K., Niizeki, Y., Suzuki, T., Sasaki, T., 2009, “The Actual Size Steam Turbine Development Facility”, Proceedings of the International Confernce on Power Engineering-09(ICOPE-09), Vol.3, pp.365-370